Piezoeletric Current from x-Cut Quartz Subjected to Short-Duration Shock-Wave Loading*

R.A. Graham and G.E. Ingram
Sandia Laboratories, Albuquerque, New Mexico 87115
(Received 9 August 1971)

When an x-cut quartz disk is subjected to an impulsive load, the piezoelectric current in an external short circuit is ordinarily an accurate time-resolved replica of the stress history at the input electrode. Recently, it has been observed that stress pulses whose durations are less than the shock-wave transit time through the disk sometimes produce anomalous current-vs-time responses. In the present work, x-cut quartz disks are subjected to stress pulses of six different durations and with amplitudes from 9 to 29 kbar. Carefully controlled accurately known pulses are applied to the samples by the impact of projectile-mounted quartz disks of various thicknesses. The piezoelectric current accompanying each stress pulse is continuously monitored as the pulse propagates through the sample disk. It is found that the anomalous current is a consequence of shock-induced conductivity in the region of the quartz disk that has been shock loaded and subsequently unloaded to a lower stress value. The threshold for conductivity is found to depend upon both stress amplitude and pulse duration. The threshold is further determined to be controlled both by a critical unloading stress value and by a critical electric field value. The critical unloading stress value is found to be 11.2 ± 0.7 kbar, and the critical electric field is found to be $(2.8 \pm 0.3) \times 10^5$ V/cm.

I. INTRODUCTION

When an x-cut quartz disk is subjected to shock-wave loading, the piezoelectric polarization produces a current in an external circuit connected between electrodes on the two faces of the disk. In previous papers[1-14] various characteristics of this current have been described for shock loading from 2 to 300 kbar. It has been shown[4,6,10] that in a linear approximation, independent of the wave profile, the short-circuited current $i(t)$ is given by the relation

$$i(t) = (kA/t_0)\,\sigma(t), \qquad 0 < t < t_0, \tag{1}$$

where k is a piezoelectric current coefficient, A the area of the charge-collecting electrode, t_0 the time required for a shock front to traverse the quartz disk at the adiabatic sound speed of 5.72 mm/μsec, and $\sigma(t)$ the stress history at the input electrode. This linear approximation is the basis for a time-resolving quartz stress gauge that has been widely used for stress measurements up to about 25 kbar. The wide use of this "Sandia quartz gauge" as a shock-profile detector is largely a result of its ability to respond accurately to stress pulses of *arbitrary profile* within restricted stress ranges.

Recently, several investigators reported that quartz disks, constructed and used as quartz gauges, *sometimes* exhibited responses that were grossly different from those predicted by Eq. (1), when they were subjected to stress pulses with durations less than the wave transit time t_0 in the gauge. Typical of these "anomalous" responses is that produced by subjecting the gauge to a stress wave with unloading, as shown in Fig. 1. In this record a very large anomalous tail, i.e., large positive excursion in current, occurs 800 nsec after first signal, even though the stress at the input face of the gauge is known to be almost zero at this time. Observation of anomalous responses on unloading raises serious questions as to the applicability of Eq. (1) when stress pulses involving unloading are encountered.[15]

The present paper describes an experimental and theoretical study of the characteristics of x-cut quartz disks employed in the Sandia quartz gauge configuration which have been subjected to short-duration stress pulse loading. As previously reported,[11] the "anomalous tail" is found to be due to a shock-induced conductivity in the region of the disk which experiences stress unloading. The experimental arrangement used to study the piezoelectric response will be presented, followed by a description of the results. These results will then be analyzed with an electrostatic theory. The phenomenological observations will then be used to propose physical mechanisms responsible for shock-induced conductivity of x-cut quartz.

II. EXPERIMENTAL ARRANGEMENT

The experimental configuration used in the present investigation is a modification of the impact configuration developed by the authors, used for the previous piezoelectric response studies of quartz,[12-14] and widely applied to other shock-loading investigations.[13,14,16] Preliminary analysis showed that both stress amplitude and pulse duration were potentially significant variables. Hence, the principal experimental problem was to achieve short-duration stress pulses, with amplitudes which are precisely specified at all times. The techniques for planar impact experiments with long-duration stress pulses are highly developed, but the short-duration loading has not been employed extensively; hence, new methods were developed to achieve the precision and control required.

The impact configuration shown in Fig. 2 is designed to achieve the symmetric impact of a projectile-mounted x-cut quartz disk (called a flier), upon an x-cut quartz disk mounted on the muzzle of a compressed gas gun. The velocity of the projectile is measured at three locations terminating at the impact plane. The gun barrel is evacuated so that gas pressure does not increase between the impacting surfaces.

For this symmetric impact condition, the particle velocity u imparted upon impact into both the flier and sample is exactly

$$u = \tfrac{1}{2} u_0, \tag{2}$$

where u_0 is the velocity of the flier at impact. Thus, the input to the sample is known to the accuracy to which the flier velocity is measured.

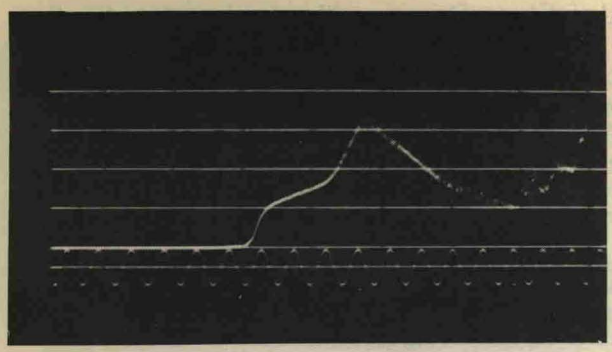

FIG. 1. Current-vs-time response observed from a quartz gauge subjected to a stress pulse propagating through a steel sample. Time increases from left to right; the timing wave has a period of 100 nsec. The maximum stress amplitude is 25 kbar. The shape of the stress pulse is determined by the elastic-plastic response of the steel sample and the unloading of stress late in time. An anomalous increase in current 800 nsec after first signal cannot be accounted for with Eq. (1). This record was obtained by Stanton under conditions as reported in Ref. 15.

The present investigation was accomplished with greatly improved accuracy in the velocity measurement compared to that previously reported.[6] The accuracy of a single velocity measurement, as calculated from the accuracies of the displacement and the time measurements, is ±0.02%. Three measurements of projectile velocity are accomplished on each experiment. The standard deviation of an individual velocity measurement from the mean value of the three velocity measurements on a particular experiment is 0.03%, when all the experiments in this paper are considered as a group. This indicates that the projectile velocity is constant for an interval of travel before impact and that the quoted impact velocities are precise to 0.1%, with 99% confidence limits.

The stress or particle velocity is varied by achieving various flier velocities; the pulse duration is varied by using fliers of different thicknesses which produce pulse durations proportional to their thicknesses. The principal problem is to achieve a precisely aligned impact surface on the thin flier which is accelerated down the gun barrel. The surface of the flier disk which is opposite to the impact face is unsupported and open to the vacuum in order to achieve a precisely specified stress after the stress pulse is reflected from this surface. Flier thicknesses from 0.65 to 2.5 mm were used in the experiments and propelled to velocities up to 0.4 mm/μsec. To prevent cracking due to excessive vibrations as the flier is accelerated down the barrel, the fliers were mounted as detailed in Fig. 2.

The median value of "tilt", i.e., misalignment achieved between impacting surfaces, was 500 μrad for the thin flier experiments. The value is calculated from the observed rise times of the quartz responses assuming that the flier and sample impact surfaces are planar. The thick impactors used in four experiments achieved mean tilt values of 200 μrad.

Excessive peak accelerations are minimized by the long-barrel (27 m) compressed gas gun[17] which allows the use of relatively massive projectiles. It was also found that the use of helium gas as a driver, as opposed to air, reduces deformations to the flier; presumably because lower driving pressures are utilized to achieve the same terminal velocity.

The Sandia quartz gauge configuration is designed to permit measurements from that portion of the shock-loaded quartz disk in which both the mechanical and electrical fields are precisely one dimensional. As shown in Fig. 2, this is accomplished with an electrode configuration consisting of an inner electrode and an outer annular guard-ring electrode. The width of the outer electrode is at least 1.5 times the thickness of the disk. The insulating gap separating the inner and outer electrode is nominally 0.09 mm wide; field perturbations due to the insulating gap are not detectable until the shock front approaches to within a distance equal to the width of the gap.[18] Furthermore, the insulating gap area is less than 3% of the inner electrode area, so that local field perturbations are negligible compared to the total area.

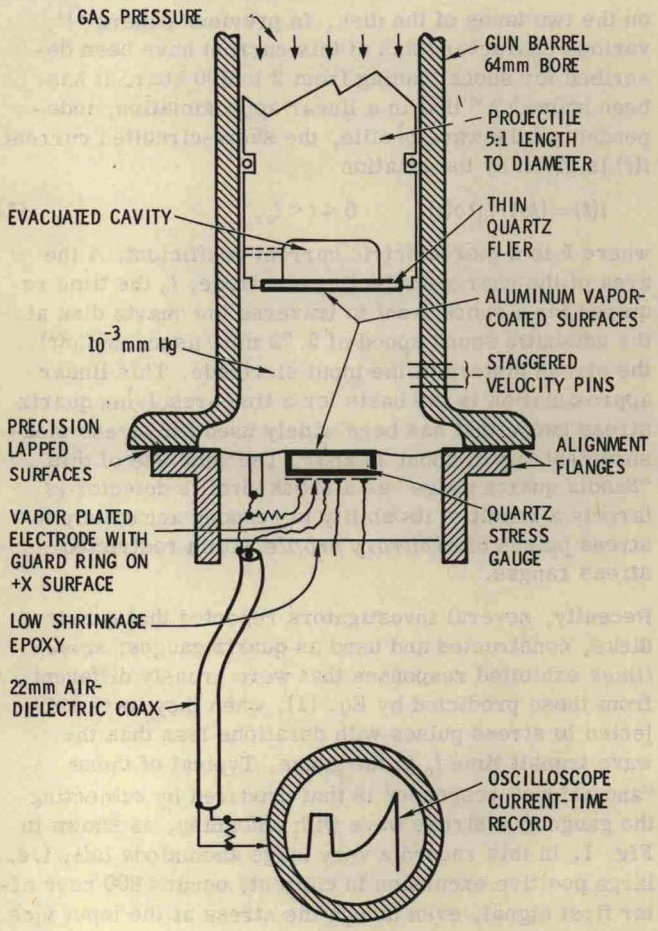

FIG. 2. Experimental configuration used to impart well-defined short-duration shock loading to the samples. Thin x-cut quartz fliers mounted on the projectile are impacted upon x-cut quartz samples to produce an input particle velocity which is known to ±0.1%. Various pulse durations are achieved by fliers of different thicknesses, and various stress amplitudes are achieved by impacts at different velocities.

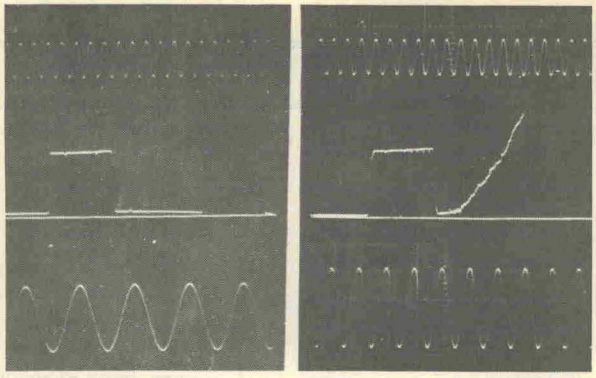

(a) (b)

FIG. 3. Typical current-time responses of x-cut quartz gauges subjected to short-duration stress pulses include those loaded below the threshold for anomalous response (a) and those loaded above the threshold of anomalous response (b). For both records, time increases from left to right. The response shown in (a) is normal in all respects; the current jumps to a value upon impact and falls to zero upon unloading. Even though the record in (b) shows a normal response until unloading occurs, a large positive excursion of current is observed late in time when the stress at the input electrode is zero. The transit time for these records is 1.11 μsec and the relative pulse durations are both 0.41. The stress applied is 9.42 kbar in (a) and 19.0 kbar in (b). Timing and voltage calibrations are shown above and below the signal traces.

Considerable care was used in the construction and inspection of each sample gauge used in the present investigation. The gauges were constructed with nominal specifications as previously given[6]; however, improved fabrication techniques[14] permitted improved performance. The guard-ring configuration was sandblasted into the plus x electrode of the quartz disk and inspected both optically and electrically. The electrode on the impact face was temporatily removed so that each disk could be inspected for inclusions in the quartz disk. Acmite inclusions[19] were found to be excessive in many disks; however, all disks used in these experiments were selected for low acmite concentrations. The open-face inspection also permitted examination of the solder connection to the rear electrode for signs of cracking due to thermal stresses. The bond of the Epoxy to the lateral surfaces and to the insulating gap was also inspected through the open face. After inspection and assembly, the impact-face electrode was vapor plated with aluminum.

Impact alignment was controlled by rigidly and precisely controlling all tolerances which can lead to misalignment. The flier is attached to the projectile with a perpendicularity of less than 50 μrad. The 28-cm-long projectile is fit to the bore of the barrel to within 2.5×10^{-3} cm on the diameter. The alignment flange on the muzzle is lapped flat and is perpendicular to the bore to within 30 μrad. The perpendicularity and parallelism of the specimen and projectile are measured for each experiment. The alignment flange is lapped frequently and the surface kept under careful scrutiny for minute damage. More details of these alignment control techniques are given in a recent publication.[14]

The current pulses from the gauges were recorded on Tektronix 585 or 454 oscilloscopes. Air dielectric cable, $\frac{7}{8}$ in. in diameter, is used for signal transmission from the gauge to the oscilloscope. The electrical impedances of cables, connectors, and terminators were checked for equivalence with a time-domain reflectometer. A newly developed pulse calibrator was used in the later part of the investigation. Important details of this instrumentation are also given in our recent publication.[14]

III. RESULTS

Two typical current-vs-time records obtained from shock-loaded sample gauges are shown in Fig. 3. Both experiments were conducted with the same flier and gauge thicknesses. The record at the lower stress, Fig. 3(a), is normal in all respects and corresponds with that expected from Eq. (1). On the other hand, the record at the higher stress shows a pronounced anomalous tail which cannot be predicted from Eq. (1) but has been found to be typical of responses well above an input stress threshold. The existence of an input stress threshold for the anomalous response can be deduced from these two experiments; however, determination of the precise value for this threshold requires more data in which both stress and pulse duration T_0 are varied in the immediate neighborhood of the threshold. Accordingly, the input stress threshold for anomalous response was investigated at six different pulse durations with impact configurations as tabulated in Table I. Experiments involving long pulse duration, i.e., $T_0 > t_0$, were also conducted on $-x$ orientation disks when similarities were discovered between the previously investigated[5-9] "$-x$ anomaly" and the present "short-pulse anomaly."

Table I includes nominal values for the relative pulse duration $\overline{T}_0/t_0 = 2l_f/l_t$, where $\overline{T}_0$ is the time for the stress pulse to complete a round trip through the unstressed thickness l_f of the flier and t_0 is the one-way transit time through the unstressed sample thickness l_t. Although these values are correct to a few percent, the exact values for the relative pulse durations depend upon the exact values of thickness and to a secondary extent upon the particle velocities and the loading and unloading wave velocities in quartz.

TABLE I. Summary of impact configurations.

Configuration	Flier thickness (mm)	Gauge thickness (mm)	Relative pulse duration $\overline{T}_0/t_0$—nominal
A	0.65	8.58	0.152
B	0.65	6.35	0.205
C	1.31	8.58	0.305
D	1.31	6.35	0.413
E	1.94	6.35	0.611
F	2.56	6.35	0.806
G	>6.4	6.35[a]	>1.0

[a] The gauges in configuration G were constructed in the $-x$ orientation, i.e., the guard ring was constructed in the $-x$ electrode and the impact occurred on the $+x$ electrode.

TABLE II. Summary of experiments.

Shot No.	T_0/t_s	Tilt (μrad)	u[a] (mm/μsec)	σ[b] (kbar)	Response
532	0.152	260	0.1883	28.5	small anomaly
529	0.152	90	0.1925	29.2	anomaly
476	0.205	1960	0.1314	19.9	normal
478	0.205	5850	0.1555	23.6	normal
477	0.205	920	0.1668	25.3	small anomaly
490	0.308	770	0.0975	14.8	very small anomaly
488	0.310	870	0.1102	16.7	anomaly
487	0.307	1030	0.1187	18.0	anomaly
430	0.412	150	0.0622	9.42	normal
475	0.413	425	0.0894	13.5	very small anomaly
462	0.414	470	0.1018	15.4	small anomaly
460	0.415	380	0.1119	17.0	anomaly
431	0.415	550	0.1257	19.0	anomaly
483	0.418	1180	0.1666	25.3	anomaly
528	0.612	220	0.0761	11.5	anomaly
464	0.614	820	0.0783	11.9	normal
479	0.614	450	0.0900	13.6	anomaly
465	0.616	940	0.0981	14.9	anomaly
511	0.813	315	0.0662	10.0	normal
513	0.814	280	0.0708	10.7	anomaly
512	0.815	320	0.0800	12.1	anomaly
		thick fliers, $-x$ orientation			
463	>1.0	75	0.0685	10.4	normal
486	>1.0	450	0.0711	10.8	anomaly
473	>1.0	120	0.0736	11.2	anomaly
618	>1.0	385	0.1016	15.4	anomaly

[a] u is the input particle velocity taken as $\frac{1}{2}$ the measured impact velocity.
[b] σ is the input stress computed from the conservation of momentum relation $\sigma=\rho_0 U u$. ρ_0 is 2.65 g cm^{-3} and U is 5.72 mm/μsec.

A. Pulse Durations and Wave Velocity

Upon impact, shock waves are imparted into both the sample disk and the flier. The duration of the stress pulse imparted to the sample is controlled by the round-trip transit time of the shock wave through the flier. Since surfaces of the flier and sample are either stationary or move with the particle velocity amplitudes, the thicknesses of the disks change in time until unloading is completed. Furthermore, the transit times depend upon the velocities of both the loading and unloading wave fronts. To calculate the pulse duration and sample thicknesses after unloading, both the loading and unloading shock fronts are assumed to travel with a velocity in laboratory coordinates, U, that is independent of stress. Under this condition, $T_0=2l_f/U$ and the transit time through the stressed sample after unloading t_s is

$$t_s=t_0\left(1-\frac{u}{U}\frac{T_0}{t_0}\right). \tag{3}$$

Since the maximum value of u/U employed in this investigation is 0.034, the nominal values of T_0/t_0 are very close to the values of T_0/t_s.

The shock velocities of the wave fronts must be determined experimentally. Previous measurements have indicated that the shock velocity of x-cut quartz has a constant value to within ±1% up to a stress of 25 kbar. Unloading wave velocities have not previously been measured, however, and a small increase in wave velocity in compression will cause a larger change to the unloading wave dispersion and influence the unloading wave shape. The present experiments afford the opportunity to test the unloading wave velocity by measuring differences between the loading time and the unloading time indicated on the current-time records. If the shock velocity is dependent on stress, the unloading stress pulse will disperse or "shock up" depending on the curvature of the stress-volume relation. To the time resolution of the present measurements, about 5 nsec, there was no evidence for dispersion or "shocking up" in the loading and unloading times indicated on the experimental records. Thus, in confirmation of previous observations, the shock velocity is independent of stress values up to 25 kbar and the shock speed equals the adiabatic sound speed. The present observation gives confirmation to the constant wave velocity to an accuracy of ±$\frac{1}{2}$%.

B. Threshold for Anomalous Response

A detailed tabulation of values determined in each experiment is shown in Table II. The principal observation is the existence or nonexistence of the anomalous tail for various values of stress and relative pulse duration. The experimental conditions were chosen to investigate the immediate neighborhood of the threshold for six different pulse durations with input stresses both above and below the threshold zone.

The locations where experiments were conducted in the relative-pulse-duration vs input-stress plane are dis-

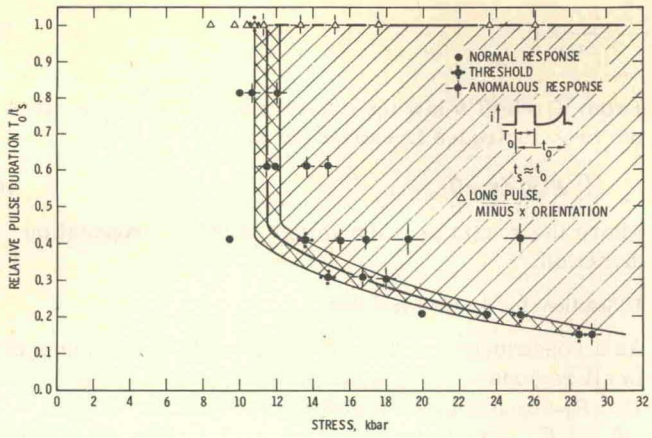

FIG. 4. Experiments at various stresses result in either a normal response or an anomalous response. The location of each experiment is shown with an indication of whether the response of the gauge is normal or anomalous. The region in which anomalous response is observed is indicated by the shaded region. The cross-hatched region indicates the area where either normal or anomalous response is observed. When the threshold conditions are grossly exceeded, larger anomalous currents are observed. For comparative purposes, experiments on $-x$-orientation long-duration loading are shown along the line $T_0/t_s = 1.0$. Data include experiments from the present work and from Ref. 9. The anomaly is not observed for $+x$ orientation long-duration loading.

played graphically in Fig. 4. The symbolism used for each experimental point in the figure indicates whether normal response or anomalous response was observed. As a secondary symbolism, the length of the lines surrounding each point indicates the extent of the anomaly; longer lines represent larger anomalies. Several experiments were conducted in the immediate vicinity of the thresholds where the current-time trace indicated only a very slight anomaly. The input-stress threshold for anomalous response is fit to the data with a cross-hatched band to indicate the zone where different values were obtained in the various experiments. The scatter in threshold values is believed to result from the variable acmite speck concentrations among the various samples. Each inclusion tends to act as a point of stress and electric field concentrations.

The threshold for anomalous response is found to have distinctly different characteristics depending upon the relative pulse duration. For relative pulse durations greater than $0.45t_s$, the anomaly is independent of relative pulse duration and is observed to occur whenever a stress of 11.2 ± 0.7 kbar is exceeded. Experiments on $-x$ orientation samples with long-pulse loading show the same threshold stress value, indicating a connection between the two phenomena.

For pulse durations less than $0.45t_s$, the threshold is found to be strongly dependent upon the pulse duration. In fact, the data indicate that with pulse durations less than $0.1t_s$, normal response will be observed at stresses as high as 40 kbar. In any event, stress pulses with durations less than $0.45t_s$ seem to exhibit an entirely different character from that of the longer duration pulses, indicating that different physical mechanisms control the anomalous response in the two pulse duration ranges. It should be emphasized that until unloading occurs, the gauges experience exactly the same conditions as in the previous long-pulse loading experiments and the gauge response is normal in all respects.

C. Residual Current Observations

After unloading and before the anomalous currents were observed, all experiments indicated a "residual" current of +1% of the maximum value. The small residual current may be a consequence of the small difference between Hugoniot loading wave velocity and adiabatic unloading wave velocity under conditions in which the polarization is not a linear function of stress. Furthermore, a tendency for the residual current to drift slightly downward late in time [see Fig. 3(a)] indicates that the one-dimensional character of the geometry is slightly perturbed very late in time.

In order to interpret the experimental observations on a physical basis, it is necessary to develop an analysis describing the electric fields for short-duration pulse loading. The conductivity of quartz has previously been shown to depend strongly upon the amplitude of the electric field and upon the polarity of the field relative to the shock front. Thus, in Sec. IV, relations for the electric fields will be developed based upon an electrostatic analysis.

IV. ELECTROSTATIC ANALYSIS

The present analysis is similar to that previously developed[6,9] for x-cut quartz under step-function loading. It is assumed that the resistivity of the piezoelectric disk is infinite. This assumption will permit explicit determination of the electric fields immediately prior to any conductivity indicated in the experimental records. In particular, the analysis will give values of the electric fields at the conductivity thresholds described in Sec. III.

The electric fields in shock-loaded quartz are a direct consequence of the piezoelectric polarization. These electric fields are uniform throughout a region of uniform polarization; but, even though the polarization is uniform, the field intensities change in time to accomodate the equal-potential condition between the electrodes. The electric field intensities at a given time depend directly on the stress amplitudes with a typical value about 10^6 V/cm at 20 kbar. Although a field of this magnitude is less than that required for dc dielectric breakdown,[20] 6×10^6 V/cm, it is a source of concern, particularly because of the large mechanical stresses to which the disk is subjected. Fortunately, the field analysis is based on straightforward physical principles and assumptions which are readily tested in the shock-loading experiments. Assumptions used in the analysis do not introduce errors larger than 1%; the principal error in the field calculation is the magnitude of the piezoelectric polarization, which according to previous work is known to within ±2.5%.

A. Electrostatic Relations

The analysis is based upon the general premise that the shock propagation speed is very much less than the propagation speed of an electromagnetic wave. Thus

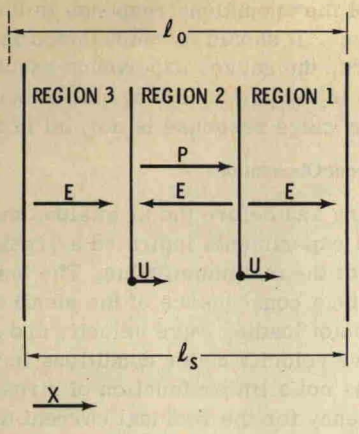

FIG. 5. Various electrical and mechanical regions along the thickness of the piezoelectric disk are shown for times when the short-duration pulse is entirely contained within the disk. Region 1, ahead of the front, is unstressed but experiences an electric field. The stress pulse in region 2 produces a region of uniform polarization proportional to the stress amplitude. Region 3, behind the unloading shock front, is unloaded to zero stress and zero polarization.

electrostatic relations are used to describe the electrical parameters, and the dynamical aspects are assumed to be controlled by the transient mechanical response. Although this situation seems reasonable, the analysis neglects an important "feedback" mechanism, electromechanical coupling, which operates to change the dynamical solution controlled by the shock propagation. This is a small (~1%) effect in quartz but can be as large as ~25% in ferroelectric materials.[21]

The problem will be restricted to the short-pulse loading problem presently being considered such that the geometric arrangement can be depicted as shown in Fig. 5. A section through the thickness of the disk, l_s, at some characteristic time after the pulse is contained within the disk shows three characteristic regions. Region 1 is the unstressed region ahead of the loading shock front; region 2 is the region of uniform stress and piezoelectric polarization with thickness UT_0; region 3 is the unstressed region behind the unloading shock front. Region 3 has been stressed to the input-stress value and subsequently reduced to zero stress. Since both the unloading and loading fronts have velocities, equal to a constant value U, region 3 has a thickness equal to $U(t-T_0)$.

The solution for the electric fields follows directly from three fundamental electrostatic relations. It is convenient to define an electric displacement D, which for our one-dimensional configuration is taken to be

$$D \equiv P + \epsilon E, \tag{4}$$

where P is the piezoelectric polarization, whose polarity is detected in compression with conventional electronic instruments, ϵ the permittivity, and E the electric field. If there is no free charge within the disk, i.e., the resistivity is infinite, Coulomb's law leads to Laplace's equation $\nabla^2\phi = 0$ which for one-dimensional conditions gives the result

$$\frac{\partial D}{\partial x} = 0. \tag{5}$$

From Kirchoff's law the external short circuit between the two electrodes is expressed as

$$\int_0^l E(x)\,dx = 0, \tag{6}$$

where the x axis is taken along the shock propagation direction.

B. Solutions for the Electric Fields

As a consequence of Eq. (5) the electric displacements in all regions are the same at a given time. Since $P_1 = P_3 = 0$, it follows immediately from Eq. (4) that $\epsilon_1 E_1 = \epsilon_3 E_3$. Assuming that $\epsilon_1 = \epsilon_3 = \epsilon_2 = \epsilon$, the unstressed permittivity,[22] it follows that $E_1 = E_3 \equiv E_{1,3}$. Thus regions 1 and 3 are identical from the electrical point of view and their thicknesses l_1 and l_3 change in time depending upon the wave speed.

The relation among the fields in the various regions is obtained from the short-circuit condition, Eq. (6), which shows that

$$E_2 l_2 + E_{1,3}(l_1 + l_3) = 0, \tag{7}$$

where l_2 equals $T_0 U$, and $l_1 + l_3 = l_s - T_0 U$. Applying Eqs. (4) and (5),

$$\epsilon E_1 = \epsilon E_3 = \epsilon E_{1,3} = P + \epsilon E_2. \tag{8}$$

Substituting the relation for E_2 from Eq. (7) into Eq. (8) gives the field in the unstressed regions:

$$E_{1,3} = \frac{+P}{\epsilon}\,\frac{T_0}{t_s}, \quad T_0 < t < t_0 \tag{9}$$

and in the stressed region

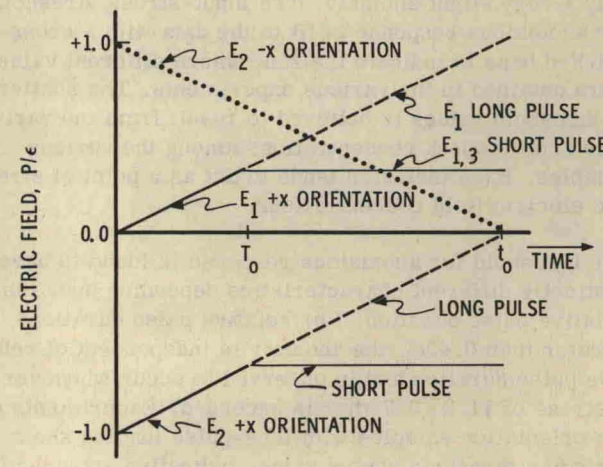

FIG. 6. Electric fields in the various regions are uniform at a given time. The field-amplitude—vs-time relations for the various regions are as indicated. Before stress unloading occurs, the fields are as indicated by the dotted line. After stress unloading occurs, the fields are constant in time and the amplitude of the field in the unloaded region is proportional to the relative pulse duration T_0/t_s. The polarity of the field in the unloaded region is such that electrons are accelerated away from a source located immediately behind the unloading wave front.

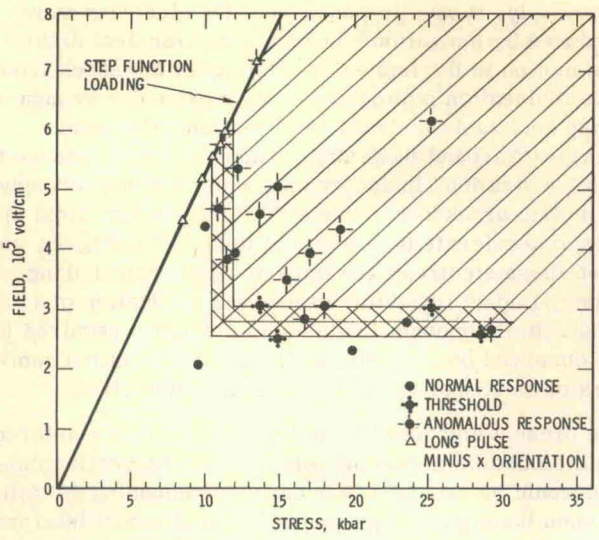

FIG. 7. Data on anomalous or normal response in Fig. 4 are transformed to the stress-vs-field plane. This representation shows that anomalous response is observed when *both* an electric field of $(2.8\pm0.3)\times10^5$ V/cm and a stress of (11.2 ± 0.7) kbar are achieved. The electric field threshold is found to be independent of stress amplitude for stresses greater than 11.2 kbar.

$$E_2=\frac{-P}{\epsilon}\left(1-\frac{T_0}{t_s}\right),\quad T_0<t<t_0 \tag{10}$$

where $t_s=l_s/U$.

These solutions for the fields have significantly different characteristics than those previously obtained for step-function loading; specifically, the solutions for step-function loading, when the displacement of the input electrode is neglected, are

$$E_2=\frac{-P}{\epsilon}\left(1-\frac{t}{t_0}\right),\quad t<t_0 \tag{11}$$

and

$$E_1=\frac{+P}{\epsilon}\left(\frac{t}{t_0}\right),\quad t<t_0. \tag{12}$$

The normalized solutions for Eqs. (9)—(12) are depicted in Fig. 6.

Until stress unloading occurs at $t=T_0$, the short pulse and step-function loading pulses produce identical responses. After the unloading wave enters the sample, i.e., when $t>T_0$, the magnitudes of the fields are constant in time. Furthermore, the magnitudes of the fields for a given polarization are directly proportional to the relative pulse durations. Thus, by introducing various pulse durations at a given stress, the amplitudes of the fields are fixed at different values.

It is important to note that the polarity of E_3 relative to the unloading front is the same as that encountered when shock-induced conductivity is observed to occur in $-x$ orientation disks under step-function loading. The shock-induced conductivity in $-x$ orientation disks was found to be a result of a free-electron source immediately behind the loading shock front.[9]

Although the solution for piezoelectric current in an external short circuit with finite conductivity in the unloaded region is not yet available, a solution for a completely shorted unloaded region, as given in the Appendix, predicts a current-time waveform similar to that observed when conditions well above the threshold are attained. Since a waveform of this sort can only be obtained by a model assuming conductivity in region 3, the anomalous response is clearly due to conduction in that region. Hence, the results will be analyzed on the premise that conductivity occurs in region 3.

The electrical field values in region 3 for each experiment are determined from Eq. (10) with results as displayed in Fig. 7. The same symbolism as in Fig. 4 is used for each experiment; each point shown indicates either normal response or an anomalous conductivity "tail". Study of the data in the field-stress plane indicates that the threshold for conductivity is achieved when an unloading stress of (11.2 ± 0.7) kbar *and* an electric field of $(2.8\pm0.3)\times10^5$ V/cm are simultaneously achieved. As stated earlier, the spread in threshold values is thought to be a result of various concentrations of acmite inclusions. Furthermore, the threshold amplitude of the electric field is observed to be independent of stress from 11.2 to 29 kbar, and the threshold stress of 11.2 kbar is found to be the same as that observed for the $-x$ orientation. We will consider the implications of these results in Sec. V.

V. DISCUSSION

Section IV demonstrated that the "anomalous" current-vs-time response observed in the short-duration shock-loading experiment is a result of shock-induced conductivity in the region of the disk that has been shock loaded and subsequently unloaded. This shock-induced conductivity is found to occur when both a threshold unloading-stress amplitude and a threshold electric field amplitude are exceeded. The threshold stress is found to have the same value as that observed for step-function loading of $-x$ orientation disks. In addition, the polarity of electric field in the unloaded region is the same as that encountered in the $-x$ orientation disks.

The polarity dependence of the conductivity in step-function loading permits the source of free electrons to be located immediately behind the loading shock front. Although the present observations do not uniquely require a source of electrons immediately behind the unloading shock front, they are consistent with the loading shock-front observations. The stress thresholds are the same for shock-induced conductivity in both loading and unloading; hence, the most consistent explanation for shock-induced conductivity in x-cut quartz is a source of electrons associated with both loading and unloading shock fronts.

It should be recalled that shock-induced conductivity is not observed in step-function loading of $+x$ orientation disks, because the field polarity impedes electron motion away from the shock front. A critical test of the location of the source of electrons is accomplished if electric field polarity is changed relative to the unloading shock front. To accomplish this an experiment was

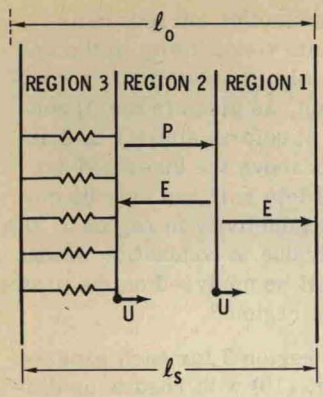

FIG. 8. Various electrical and mechanical regions along the thickness of the disk are shown when the short-duration pulse is entirely contained within the disk and the unloaded region 3 is highly conductive. This configuration would be expected to exist for stress and electric fields much greater than the observed threshold values.

conducted in which an incrementally stepped unloading wave shape was applied to a quartz gauge disk. The configuration was the same as that employed in the main part of the investigation except that the flier used to impact the quartz sample was a 1.5-mm-thick sapphire disk. Since the sapphire has a much higher mechanical impedance than quartz, the unloading occurs incrementally, unloading approximately one-half of the reflected stress amplitude in time increments equal to the round-trip transit time through the thickness of the flier. With an impact stress of 30.8 kbar, the stress was reduced to 15.9 kbar at the first unloading.

Extension of the analysis leading to Eq. (9) for incrementally stepped reductions of polarization showed that the polarity of the electric field after the first unloading was oriented so as to impede the acceleration of electrons from the unloading shock front. The current-time response from the disk showed no evidence for conductivity under these conditions. Later in time, after several unloading steps, the analysis shows that the electric field polarity reverses. When the reversal occurred and the electric field was greater than the threshold value, the observed current-time response from the disk was observed to have the same "anomalous" response as was observed for the complete unloading experiments.

The results of this incrementally stepped unloading experiment confirm that the unloading shock front is a source of electrons in a similar manner as observed for loading shock fronts. Furthermore, roughly the same threshold conditions are applicable to incremental unloading as for a shock front which causes complete unloading.

The principal requirements for a physical model to explain the shock-induced conductivity of x-cut quartz are (i) a mechanism for a threshold electric field for conductivity which is more than an order of magnitude lower than the electric field required for dielectric breakdown at atmospheric pressure, and (ii) a mechanism providing a source of electrons at the shock front under conditions in which the elastic strain energy and thermal energy are orders of magnitude too low for ionization of impurities. The experimental observation that the source of electrons is located immediately behind the shock front further restricts the model; the source is apparently transient and closely coupled to the shock fronts.

Previously, it was proposed[5] that the electrons were produced by ionization accompanying transient dislocation motion in the immediate vicinity of the shock front. This dislocation motion need not be extensive enough to cause detectable inelastic deformation. The local energies[23] around these dislocations are large enough to cause ionization. In accordance with presently accepted dielectric breakdown models,[24-26] the electric field then acts to accelerate the electrons to higher energies, and when these electrons are impacted upon neighboring atoms, impact ionization causes the production of a substantially enhanced number of electrons required for the observed conductivities. Hence, only limited numbers of electrons are required at the shock front.

The present unloading response observations reinforce the dislocation motion proposal, since dislocation motion would be expected to occur upon unloading as well as upon loading. The proposed physical model interprets the 11.2-kbar threshold stress as the threshold stress to cause limited dislocation motion in the shock fronts; the threshold field value of 2.8×10^5 V/cm is interpreted to be that field required to achieve impact ionization in x-cut quartz. This threshold electric field is a factor of about 30 lower than that required for dielectric breakdown at atmospheric pressure. The present observations indicate that the dielectric breakdown of x-cut quartz at atmospheric pressure is initiated by field ionization of impurities, whereas breakdown under shock compression is initiated by stress-induced ionization through dislocation motion above a critical stress value. The present model has the feature that the electric field threshold is independent of stress amplitude, in agreement with an important feature of the experimental observations.

In comparison to the present observations, it should be observed that analysis of the current-time waveforms previously reported for the $-x$ orientation experiments showed recovery of low values of conductivity when the electric field was reduced in amplitude.[9] Analysis of this recovery process showed that the recovery occurred when the electric field fell below $(1.9\pm0.5)\times10^5$ V/cm. This field amplitude was observed to be independent of stress amplitude, and the value is close to that observed in the present investigation. The experimental conditions of the present investigation are much better controlled and, unlike the analysis of the $-x$ orientation data, the present analysis does not depend critically upon details of the current-time wave shape. Hence, the electric field amplitudes of the present investigation are more accurately known than those obtained in the $-x$ orientation analysis. In any event, both the threshold electric field required to induce conductivity and the threshold electric field required to recover low conductivity values are observed to be independent of the amplitude of the stress.

The extent to which the present observation can be applied to stress pulses of arbitrary wave shape remains to be determined. The stepped unloading experiment reported in the present work and the widespread observation of anomalous response by various investigators who have subjected quartz disks to various wave shapes, demonstrate that the existence of the conductivity is not

restricted to shock fronts. However, determination of the extent to which the same threshold values for stress and field are applicable requires a more general analysis of the electric fields in a piezoelectric disk subjected to a stress pulse of arbitrary shape. The development of this analysis is in progress.

VI. CONCLUSIONS

The conclusions of the present work are:

(i) "Anomalous" current-time wave shapes observed from x-cut quartz after stress unloading in short-duration loading experiments are a result of shock-induced conductivity in the unloaded region of the quartz disk.

(ii) Shock-induced conductivity requires a threshold unloading stress of (11.2 ± 0.7) kbar as well as a threshold electric field of $(2.8 \pm 0.3) \times 10^5$ V/cm.

(iii) The threshold electric field for conductivity is found to be independent of stress amplitude for stress amplitudes greater than the threshold value.

(iv) Shock-induced conductivity is triggered by a source of electrons immediately behind shock fronts whose stress amplitudes exceed the threshold value.

(v) The electrons appear to result from strain-induced ionization accompanying transient dislocation motion in the shock front.

(vi) It appears that the electric field acts to accelerate these source electrons to high energies which causes impact ionization and electron cascades.

(vii) The "short-pulse anomaly" observed with $+x$ orientation disks and the "$-x$ anomaly" observed in $-x$ orientation disks are basically the same phenomenon requiring electric fields of the proper polarity; in the former situation the unloading front acts as a source of electrons, while in the latter situation the loading front acts as a source of electrons.

(viii) Finally, the unloading stress front in x-cut quartz shows no evidence for dispersion in the stress range from 0 to 25 kbar.

ACKNOWLEDGMENTS

The authors are pleased to acknowledge discussions with W.B. Benedick on the acmite speck problem in quartz and the cooperation of Sawyer Research Prod. and the Valpey-Fisher Corp. for their efforts in improving the quality of the quartz disks. Numerous people were very cooperative in allowing us to examine their quartz gauge records for evidences of anomalous responses. These include: P.L. Stanton, E.A. Ripperger, T. Meagher, C. Stoll, C.M. Percival, Capt. P. Crotwell, Capt. Dave Carlson, and Capt. L. Carlton. Discussions with T. Meagher and P.L. Stanton were instrumental in calling the authors' attention to the anomalous responses.

APPENDIX

Equations will be derived for the current from x-cut quartz disks subjected to short-duration shock loading while experiencing a low resistivity value through the unloaded stress region.

The general configuration is as shown in Fig. 8. The conditions are the same as in the main body of the text, except that region 3 is conductive. With the same electrostatic relations utilized in the text,

$$E_1 l_1 + E_2 l_2 = 0; \tag{A1}$$

hence,

$$E_2 = -E_1 (t_0 - t)/T_0 . \tag{A2}$$

Applying Eq. (5), it follows that

$$\epsilon E_1 = P + \epsilon E_2, \tag{A3}$$

which, when combined with Eq. (A2), gives the result that

$$E_1 = (P/\epsilon)\,[T_0/(T_0 + t_0 - t)], \quad t > T_0. \tag{A4}$$

Solving for the current from the relation

$$i = A \frac{dD}{dt}, \tag{A5}$$

we find that

$$i = PAT_0 (T_0 + t_0 - t)^{-2}, \quad t > T_0 < t_0. \tag{A6}$$

Note that when $t = T_0$, $i_{T_0} = PAT_0/t_0^2$, and when $t = t_0$, $i = PA/T_0$. For the highest field and stress achieved in the experiments, current-time responses described by (A6) were observed. These solutions are similar to those obtained for the three-zone model of shock-loaded quartz.[4]

---

*Work supported by the U.S. Atomic Energy Commission.

[1] F.W. Neilson and W.B. Benedick, Bull. Am. Phys. Soc. 5, 511 (1960).
[2] R.A. Graham, Bull. Am. Phys. Soc. 5, 511 (1960).
[3] R.A. Graham, J. Appl. Phys. 32, 555 (1961).
[4] F.W. Neilson, W.B. Benedick, W.P. Brooks, R.A. Graham, and G.W. Anderson in *Les Ondes de Detonation* (Editions du Centre National de la Recherche Scientifique, Paris, 1962); also Sandia Corporation Report No. SCR-416, 1961 (unpublished).
[5] R.A. Graham, J. Appl. Phys. 33, 1755 (1962).
[6] R.A. Graham, F.W. Neilson, and W.B. Benedick, J. Appl. Phys. 36, 1775 (1965).
[7] O.E. Jones, Rev. Sci. Instr. 38, 253 (1967).
[8] R.W. Rohde and O.E. Jones, Rev. Sci. Instr. 39, 313 (1968).
[9] R.A. Graham and W.J. Halpin, J. Appl. Phys. 39, 5077 (1968).
[10] O.E. Jones, F.W. Neilson, and W.B. Benedick, J. Appl. Phys. 33, 3224 (1962).
[11] R.A. Graham and G.E. Ingram, Bull. Am. Phys. Soc. 13, 1660 (1968).
[12] R.A. Graham, Rev. Sci. Instr. 32, 1308 (1961).
[13] R.A. Graham, J. Basic Engr. 89, 911 (1967).
[14] G.E. Ingram and R.A. Graham, in Fifth Symposium on Detonation, 1970 (unpublished).
[15] The anomalous responses were first reported by P.L. Stanton, a Ph.D. thesis (University of Texas, 1968) (unpublished), in explosively driven flier plate experiments; in 1968 from T. Meagher (private communication), Kaman Aviation, Nuclear Products Div., Colorado Springs, Colorado in compressed gas gun experiments; J.B. Webster, M.S. thesis (Air Force Institute of Technology, 1965) (unpublished); and C.E. Harris, M.S. thesis (Air Force Institute of Technology, 1966) (unpublished), both in compressed gas gun experiments; from various Sandia Laboratories employees (private communication), from experiments in which short-duration

stress pulses were induced in solids by the deposition of pulsed x rays in underground nuclear tests at the Nevada Test Site.

[16]C.H. Karnes, in *Mechanical Behavior of Materials Under Dynamic Loads*, edited by U.S. Lindholm (Springer-Verlag, New York, 1968).

[17]S. Thunborg, G.E. Ingram, and R.A. Graham, Rev. Sci. Instr. **35**, 11 (1964).

[18]J.R. Freeman, Sandia Laboratories Report No. SC-RR-69-55, 1969 (unpublished).

[19]Acmite, sodium-iron silicate, is formed in the quartz-crystal hydrothermal growth process. Fine specks of acmite tend to become trapped in the growing crystal. These acmite specks range from sizes barely visible to the unaided eye up to 0.25 mm in size. New quartz specifications call for visual counts of the number of acmite specks per unit volume on the finished quartz disks and control of the maximum number and size of the acmite specks. New growth techniques have now reduced typical acmite concentrations. See B. Sawyer, Sawyer Research Prod. Report, Eastlake, Ohio (unpublished).

[20]A. von Hippel and R.J. Maurer, Phys. Rev. **59**, 820 (1941).

[21]O.M. Stuetzer, J. Acoust. Soc. Am. **42**, 502 (1967).

[22]Previous investigations (Ref. 6) have shown that the permittivity increases by only a few tenths of one percent for an applied stress of 20 kbar. Hence, the change is negligible for the present problem. The analysis shown here can readily be extended to various permittivity values.

[23]H.G. van Bueren, *Imperfections in Crystals* (North-Holland, Amsterdam, 1961).

[24]S. Whitehead, *Dielectric Breakdown of Solids* (Clarendon, Oxford, England, 1953).

[25]J.J. O'Dwyer, *Theory of Dielectric Breakdown of Solids* (Oxford U.P., Oxford, England, 1969).

[26]N. Klein, in *Advances in Electronics and Electron Physics*, edited by L. Marton (Academic, New York, 1969).